Patterns of retropharyngeal lymph node metastasis in nasopharyngeal carcinoma.

Qifeng Hua[1], Jianjun Zheng[1], Bibo Hu[1], Ming Shu[2*], Li Shen[1], Jiebo Chen[3]

[1]Department of Radiology, Ningbo No.2 Hospital, Ningbo 315010, PR China

[2]Department of the Third Surgery, Ningbo No.2 Hospital, Ningbo 315010, PR China

[3]Department of Radiation Therapy, Ningbo No.2 Hospital, Ningbo 315010, PR China

Abstract

This study aimed to investigate the patterns of retropharyngeal lymph node (RLN) metastasis in patients with nasopharyngeal carcinoma (NPC). Sixty-two patients with NPC underwent nasopharyngeal magnetic resonance imaging. Magnetic resonance images were reviewed collectively by the research team. Nodal involvement was classified according to the Radiation Therapy Oncology Group nodal classification guidelines. Locations of the involved RLNs were recorded, and the relationships of RLN metastasis with primary tumor extension and clinical stage were analyzed. Among 62 patients with NPC, 47 (75.8%) exhibited level IIb nodal metastasis, and 39 (62.9%) had RLN metastases. Overall, 60 metastatic RLNs were detected. The center, cranial, and caudal borders of metastatic RLNs respectively included four (6.7%), 17 (28.3%) and three (5.0%) lymph nodes in the occipital bone; 45 (75.0%), 40 (66.7%), and 33 (55.0%) lymph nodes in the first cervical vertebra (C1); 10 (16.7%), three (5.0%), and 21 (35.0%) lymph nodes in the second cervical vertebra (C2); and zero (0.0%), zero (0.0%), and three (5.0%) lymph nodes in the third cervical vertebra (C3). The incidence of RLN involvement did not increase with the incidence of primary tumor invasion to the parapharyngeal space, prevertebral muscle, oropharynx, nasal cavity, skull base, paranasal sinuses, and cavernous sinus. The incidence of nodal metastasis among patients with NPC was highest at the cervical lymph node level IIb, followed by the RLNs. There was a linear decrease in the incidence of metastatic lateral RLNs from levels C1 to C3.

Introduction

Nasopharyngeal carcinoma (NPC) is one of the most common types of malignant tumors, and, as the nasopharynx is rich in lymphatic drainage, 60-90% of affected patients present with lymph node metastasis prior to treatment. Treatment efficacy depends on tumor T stage, N stage, histological type, adjacent invasion, tumor size, and selected treatment programs [1]. Currently, radiotherapy is the mainstay of treatment for NPC, and the overarching principles of lymph node metastasis have been a significant factor in radiation field design. A study by Kato et al. indicated that magnetic resonance imaging (MRI) exhibited a significantly better ability than computed tomography (CT) in detecting retropharyngeal lymph node (RLN) metastasis [2]. Soft tissue is more readily visible on MRI; hence, MRI can present lymph node metastasis and NPC clearly and completely. MRI has been widely applied for the diagnosis of NPC, largely because it decreases radiation exposure. In 2008, Liao [3] reported a significant difference between CT and MRI in distinguishing invasion of the base of the skull (CT 31. 0%, MRI 52. 6%) in 420 patients diagnosed with NPC. Zhan et al. [4] found that the positive rates of invasion were 48.3% and 33.3% using MR and CT, respectively. Therefore, MRI has more advantages in distinguishing invasion of the base of the skull, and it can be used to accurately estimate invaded range and accurately sketch the tumor target.

In this study, the principles of RLN metastasis in NPC were analyzed using MRI. According to the literature, the cervical lymph nodes and RLNs are the most common sites of metastasis. Although pharyngeal lymph node metastasis is common in NPC, its prognostic value is not clear, and the current staging system does not specify whether RLNs should be subject to T or N staging. Therefore, studies of the principles of RLN metastasis are important not only when determining regions that should be targeted with radiotherapy in cases of NPC, but also for clarifying their prognostic value in staging systems.

Materials and Methods

Clinical data

Sixty-two patients with pathologically confirmed NPC underwent initial treatment at our hospital between November 2009 and April 2010. The patients had a median age of 49 years, and a male: female ratio of 3.4:1 (48 men, 14 women). Before treatment, all patients underwent nasopharyngeal MRI, chest radiography or CT, and abdominal B-ultrasonography. Patients with stage T3-4 disease, lymph node diameter >4 cm, or supraclavicular lymph node metastasis also underwent whole-body bone scans. This study was conducted in accordance with the declaration of Helsinki. This study was conducted with approval from the Ethics Committee of Ningbo No.2 Hospital. Written informed consent was obtained from all participants.

MRI examination

A SIEMENS 1.0 T device (Siemens, Munich, Germany) and head and neck coil were used for dual gradient MRI as follows: for cross-sectional and sagittal T1-weighted imaging, the repetition time (TR) was 400-500 ms and the echo time (TE) was 10-15 ms; for cross-sectional T2-weighted imaging, the TR and TE were 4000-5000 ms and 80-100 ms, respectively. Imaging was repeated after an intravenous injection of gadopentetic acid contrast agent (Gd-DTPA; 0.1 mmol/kg); specifically, cross-sectional and coronal T1-weighted fast spoiled gradient echo fat suppression sequence scans (TR: 150-250 ms, TE: 2-10 ms) were performed using the following settings: cross-sectional thickness: 6 mm; interlayer spacing: 1 mm; sagittal and coronal plane thickness: 4 mm; and interlayer spacing: 1 mm.

Image reading

All MRI scans were read collectively by two head and neck radiologists. The evaluation criteria for lymph node metastasis were as follows: 1) smallest neck lymph node diameter ≥ 10 mm; 2) minimum lateral group RLN diameter ≥ 5 mm; 3) any visible RLN in the outer group; 4) lymph nodes distributed in a cluster; and 5) presence of central necrosis or invasion beyond the lymph node capsule. The cranial and caudal borders and center position (reference: cervical spine) were recorded. Cervical lymph node positions were determined using the methods suggested by Roy et al. [5].

Statistical analysis

All data were entered into the SPSS 11.5 software (SPSS, Inc., Chicago, IL, USA), and the chi-square and Fisher's exact tests were used to analyze the relationships among RLN metastasis, primary tumor, surrounding tissue involvement, and clinical staging. A P value<0.05 was considered statistically significant.

Results

Overall situation of lymph node metastasis

Of the 62 evaluated patients, 39 (39/62, 62.9%) had RLN metastases, 47 (47/62, 75.8%) had level IIb lymph node metastases, and 54 (54/62, 87.1%) had some type of lymph node metastasis. Four patients (4/62, 6.5%) had only RLN metastasis, 15 (15/62, 24.2%) had only cervical lymph node metastasis, and 36 (36/62, 58.1%) had both RLN and cervical lymph node metastases. The rate of RLN metastasis was significantly lower than that of cervical lymph node metastasis (62.9% *vs.* 82.3%, P=0.028).

RLN metastasis

Of the 39 patients with RLN metastasis, 22 (22/39, 56.4%) had unilateral RLN metastasis, and 17 (17/39, 43.6%) had bilateral RLN metastasis. Sixty metastatic RLNs were located in the outer group; no lymph node enlargement was visible in the inner group. The average minimum and maximum transverse diameters and longitudinal length of the metastatic RLNs were 1.5 ± 0.6 cm (range: 0.5-3.6 cm), 1.6 ± 0.7 cm (0.8-4.8 cm), and 2.5 ± 1.4 cm (0.9-6.8 cm), respectively. The center and cranial and caudal borders (reference: cervical spine) in the 60 patients are shown in Table 1. Overall, the RLN metastasis rate gradually reduced from the first cervical vertebra (C1) to the third cervical vertebra (C3) level (Fisher's exact test, P=3.17 × 10^{-4}, P<0.05).

Table 1. *Location of 60 metastatic RLN.*

Locations on MR	Central location of lymph node	Cranial border of lymph node	Caudal border of lymph node
Occipital bone	4 (6.7%)	17 (28.3%)	3 (5.0%)
The first cervical vertebra	45 (75.0%)	40 (66.7%)	33 (55.0%)
The second cervical vertebra	10 (16.7%)	3 (5.0%)	21 (35.0%)
The third cervical vertebra	0 (0%)	0 (0%)	3 (5.0%)

Of 39 patients with 60 RLNs, 20 (20/39, 51.3%) had one RLN, 17 (17/39, 43.6%) had two RLNs, and two (2/39, 5.1%) had three RLNs. A total of 18 RLNs (18/60, 30%) had central necrosis. The diameters of necrotic RLN ranged from 0.5 cm to 3.6 cm. No necrosis was found in RLNs with diameters<0.5 cm.

Relationship between lymph node metastasis and tumor invasion site

Data describing the relationship between lymph node metastasis and tumor invasion site are presented in Table 2. Notably, RLN metastasis did not correlate with invasion of the pharyngeal space, nasal cavity, oropharynx, palate sail muscle, head longus, pterygoid and wing muscle, skull base, pterygopalatine fossa, infratemporal fossa, paranasal sinuses, eye orbital, cavernous sinus, or other sites. Additionally, we

did not observe a relationship between RLN metastasis and staging, which might be attributable to the small number of cases (Table 3).

Table 2. Relationship between RLN metastasis and primary NPC involved scope.

Tumor involved sites	Number of positive RLN (%)			
	No violation	Violation	χ^2 value	P value
Parapharyngeal space	18/32 (56.3)	21/30 (70.0)	1.255	0.263
Sail palate muscle	22/33 (66.7)	18/29 (62.1)	0.143	0.706
Oropharynx	37/58 (63.8)	2/4 (50.0)	0.000	0.986
Nasal cavity	32/50 (64.0)	8/12 (66.7)	0.000	1.000
Prevertebral muscle	26/41 (63.4)	13/21 (61.9)	0.014	0.907
Wing extrafusal	35/54 (64.8)	4/8 (50.0)	0.174	0.676
Pterygoid an flap	33/51 (64.7)	7/11 (63.6)	0.000	1.000
Rupture hole	32/50 (64.0)	7/12 (58.3)	0.133	0.715
Slope	27/43 (62.8)	12/19 (63.2)	0.001	0.978
Foramen ovale	33/52 (63.5)	6/10 (60.0)	0.000	1.000
Temporal bone petrous apex	30/48 (62.5)	9/14 (64.3)	0.015	0.903
Pterygopalatine fossa	37/58 (63.8)	2/4 (50.0)	0.000	0.986
Sphenoid wing	34/52 (65.4)	6/10 (60.0)	0.000	1.000
Sphenoid	33/51 (64.7)	6/11 (54.5)	0.400	0.527
Ethmoid	38/59 (64.4)	2/3 (66.7)	0.000	1.000
Maxillary	37/59 (62.7)	2/3 (66.7)	0.000	1.000
Orbital apex	38/60 (63.3)	1/2 (50.0)	0.000	1.000
Cavernous sinus	35/54 (64.8)	4/8 (50.0)	0.174	0.676
Temporal fossa	37/59 (62.7)	2/3 (66.7)	0.000	1.000

Table 3. Relationship between RLN metastasis and staging.

RLN	Number of patients (%)			
	T1	T2	T3	T4
Negative	5/13 (38.5)	8/24 (33.3)	4/13 (30.8)	5/12 (41.7)
Positive	8/13 (61.5	16/24 (66.7)	9/13 (69.2)	7/12 (58.3)
	I	II	III	IV
Negative	2/2 (100.0)	7/16 (43.8)	8/26 (30.8)	6/18 (33.3)
Negative	0/2 (0.00)	9/16 (56.2)	18/26 (69.2)	12/18 (66.7)

Discussion

Radiotherapy is the treatment of choice for NPC, and it is even preferred over surgery. Therefore, it is difficult to perform pathology via lymph node dissection, and the reported 5-year post-radiotherapy survival rate among patients with NPC is as high as 83.3% [6-8]. Due to the application of intensity-modulated radiotherapy, the 5-year survival rate has improved to 78-83.3% [9-10]. Herein, all cases with long-term follow-up may be used to assess the diagnosis of lymphatic metastasis, and relevant results may validate the accuracy of lymphatic metastasis by excluding the history of other potential tumors. Therefore, it is difficult to define the relationship between pathological diagnosis and imaging performance of lymph node metastasis. Previous studies have found that RLNs shrink with age; specifically, Ng et al. [11] and Ogura et al. [12] reported that on MRI scans, the minimum RLN transverse diameters among patients aged 6-19 years, 20-38 years, and 42-74 years were 6.4 ± 1.4 mm, 4.2 ± 1.1 mm, and 3.2 ± 1.0 mm, respectively. The minimum transverse diameters of normal RLNs on MRI scans in our study were ≤ 4.5 mm. Therefore, the present study used a minimum RLN diameter ≥ 5 mm as a diagnostic criterion for metastasis. Although some authors have used central necrosis as a diagnostic criterion for RLN metastasis, we seldom observed this phenomenon in lymph nodes with small diameters. The present study suggests that these standards cannot improve the sensitivity of RLN diagnosis. In this study, 62.9% patients had RLN metastases, consistent with the rate of 63.6% reported in the literature. RLNs include the outer and inner groups; the former is located outside the pharyngeal constrictor muscle and vertebral anterior muscle and inside the internal carotid artery (Figure 1). The latter is located near the body midline, close to the posterior pharyngeal wall. In this study, all assessed RLNs were located in the outer group. Because the RLNs in the inner group were not normally visible, any visible RLNs in this group on MRI were considered metastatic; however, a previous article reported that NPC with RLN metastases in the inner group was very rare.
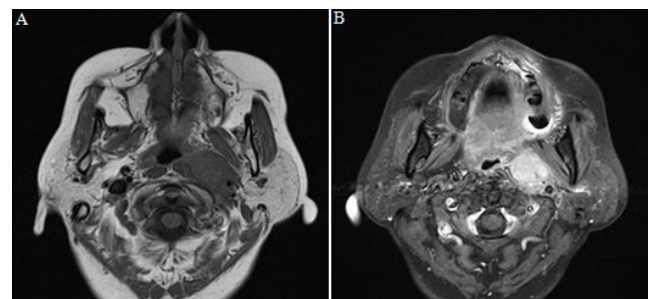

Figure 1. Schematics of RLN metastasis in outer group. A: T1-weighted MR images; B: T1-weighted fat-suppressed enhancement MR image.

King et al. [13] and Chong et al. [14] described the locations of RLNs in detail. Chong et al. [14] found that the majority of RLN metastases were located above the level of the second cervical vertebra, and King et al. [13] found that 63% of RLNs extended down to the level of the second cervical vertebra, 19% reached the second and third cervical levels, and 6% reached the level of the third cervical vertebra. Differences between the two studies were mainly attributable to differences in the methods used to record RLN positions. Wang et al. [15] described in detail the longitudinal center diameters and cranial and caudal borders in 618 patients with NPC and RLN metastases. Studies have shown that most metastatic lymph

nodes were located in the first cervical vertebral level, regardless of the center or the cranial and caudal borders, and that the RLN metastasis rate gradually decreased from the first to the third cervical vertebral levels. Som et al. [16] first proposed defining RLNs as those located under the skull base to within a 2 cm range of the skull base, according to imaging. However, Wang et al. [15] and Kao et al. [17] observed that many RLN metastases in NPC cases exceeded this range on CT, and Ogura et al. [12] and additional MRI results from the present study indicated that the range of RLNs as defined by Som et al. [16,18-20] was too small and not suitable for application to NPC. The study group also observed multiple ipsilateral RLN metastases located between the base of the skull to the lower edge of the third cervical vertebra; accordingly, the RLN irradiation range in patients with NPC should extend from the base of the skull to the lower edge of the third cervical vertebral level.
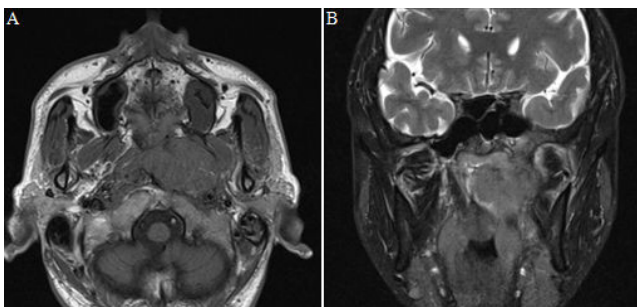

Figure 2. A) T1 B-weighted MR image; B) Coronal fat-suppressed enhancement T2-weighted MR image showed bilateral posterior RLN metastasis.

Although previous research has shown correlations between the lymphatic drainage pathway in the head and neck and the primary tumor and the location and scope of tumor invasion, the risk of RLN metastasis was found to increase when the tumor extended beyond the pharyngobasilar fascia. Liu et al. [21,22] reported a significantly lower RLN metastasis rate among T1 patients, compared to T2-4 patients (48.3% *vs.* 71.0%), and observed that RLN metastasis increased significantly when the sail palate muscle, oropharynx, prevertebral muscle, pterygoid muscle, and styloid gap were involved. Wang et al. [15] also reported that the RLN metastasis rate increased significantly with parapharyngeal space involvement, but did not increase when the nasal cavity, oropharynx, head longus, skull bone, paranasal sinuses, eye orbital, cavernous sinus, or other sites were involved. However, in the present study, we did not observe a similar relationship, which might be attributable to the small number of cases (Table 3).

The effect of RLN metastasis on NPC prognosis was inconclusive. At present, both domestic and international staging systems do not clearly define RLN etiologies, which vary among tumor centers. Given the high incidence of NPC and higher NPC metastasis rates in Southeast Asia and the southeast coastal areas of China, in-depth studies regarding the prognostic significance of the RLN metastasis rate are required. Some authors observed a higher distant metastasis

rate among patients with NPC and RLNs; however, in a CT-based study by Chua et al. [23-30], which used a transverse diameter $\geq$ 10 mm as a diagnostic criterion of RLNs, RLN metastasis was not found to have an effect on the prognosis of NPC. Among the 62 patients in this group, the vast majority of patients with RLN metastasis also had cervical lymph node metastasis (Figure 2); only four patients (6.5%) had RLN metastasis alone, and eight (12.9%) patients had no lymph node metastases. Therefore, a longer period is needed to accumulate more cases and better evaluate the impact of RLN metastasis on the prognosis of NPC during long-term follow-up.

In short, the highest rate of metastasis of NPC was observed in level IIb lymph nodes, followed by RLNs. The majority of RLN metastases were located in the outer group; metastasis in the inner group was rare. The rate of RLN metastasis decreased gradually from the first to the third cervical vertebral levels. RLN metastasis had no significant correlations with the sites of NPC involvement or staging. This finding is inconsistent with other reports from larger sample sizes. We believe that the transfer of lymphonodi retropharynici is not correlated with invaded areas in nasopharyngeal cancer and neoplasm staging. Moreover, except for specific regions in Ningbo located in the coastal city, it has certain characteristics. Despite its small sample size, this study findings support confirmation with a larger sample, which may improve radiotherapy treatment in patients with nasopharyngeal carcinoma lymph node metastasis.

Our study had some limitations. First, it was a retrospective follow-up study, and the majority of patients had no pathological diagnosis. Second, the sample size was small, and statistical errors were possible. Third, we must recognize the limitations of MRI and note that some cases had false-positive or false-negative clinical performances.

Acknowledgement

References

1. Wang Y, Zhao H, Zhang ZQ, Huang LL, Ye Y, Wang YB, Han MJ. MR imaging prediction of local control of nasopharygeal carcinoma treated with radiation therapy and chemotherapy. Br J Radiol 2014; 87: 20130657.

2. Kato H, Kanematsu M, Watanabe H, Mizuta K, Aoki M. Metastatic retropharyngeal lymph nodes: comparison of CT and MR imaging for diagnostic accuracy. Eur J Radiol 2014; 83: 1157-1162.

3. Liao XB, Mao YP, Liu LZ, Tang LL, Sun Y, Wang Y, Lin AH, Cui CY, Li L, Ma J. How does magnetic resonance imaging influence staging according to AJCC staging system for nasopharyngeal carcinoma compared with computed tomography? Int J Radiat Oncol Biol Phys 2008; 72: 1368-1377.

4. Zhang SX, Han PH, Zhang GQ, Wang RH, Ge YB, Ren ZG, Li JS, Fu WH. Comparison of SPECT/CT, MRI and CT in diagnosis of skull base bone invasion in nasopharyngeal carcinoma. Biomed Mater Eng 2014; 24: 1117-1124.

5. Roy M, Bouchard-Fortier G, Popa I, Grégoire J, Renaud MC, Têtu B, Plante M. Value of sentinel node mapping in cancer of the cervix. Gynecol Oncol 2011; 122: 269-274.

6. Xiao GL, Gao L, Xu GZ. Prognostic influence of parapharyngeal space involvement in nasopharyngeal carcinoma. Int J Radiat Oncol Biol Phys 2002; 52: 957-963.

7. McLaughlin MP, Mendenhall WM, Mancuso AA, Parsons JT, McCarty PJ, Cassisi NJ, Stringer SP, Tart RP, Mukherji SK, Million RR. Retropharyngeal adenopathy as a predictor of outcome in squamous cell carcinoma of the head and neck. Head Neck 1995; 17: 190-198.

8. Mukherji SK, Armao D, Joshi VM. Cervical nodal metastases in squamous cell carcinoma of the head and neck: what to expect. Head Neck 2001; 23: 995-1005.

9. Xiao WW, Lu TX, Zhao C, Han F, Su SF. Impact of intensity-modulated radiotherapy on the 6th edition of UICC/AJCC staging system in nasopharyngeal carcinoma. Chin J of Radiat Oncol 2010; 19: 181-184.

10. Xu T, Zhu G, He X, Ying H, Hu C. A phase III randomized study comparing neoadjuvant chemotherapy with concurrent chemotherapy combined with radiotherapy for locoregionally advanced nasopharyngeal carcinoma: updated long-term survival outcomes. Oral Oncol 2014; 50: 71-76.

11. Ng SH, Chang TC, Ko SF, Yen PS, Wan YL, Tang LM, Tsai MH. Nasopharyngeal carcinoma: MRI and CT assessment. Neuroradiology 1997; 39: 741-746.

12. Ogura I, Kaneda T, Kato M, Mori S, Motohashi J, Lee K. MR study of lateral retropharyngeal lymph nodes at different ages. Oral Surg Oral Med Oral Pathol Oral Radiol Endod 2004; 98: 355-358.

13. King AD, Ahuja AT, Leung SF, Lam WW, Teo P, Chan YL, Metreweli C. Neck node metastases from nasopharyngeal carcinoma: MR imaging of patterns of disease. Head Neck 2000; 22: 275-281.

14. Chong VF, Fan YF, Khoo JB. Retropharyngeal lymphadenopathy in nasopharyngeal carcinoma. Eur J Radiol 1995; 21: 100-105.

15. Wang XS, Hu CS, Ying HM, Zhou ZR, Ding JH, Feng Y. Patterns of retropharyngeal lymph node metastasis in nasopharyngeal carcinoma. Int J Radiat Oncol Biol Phys 2009; 73: 194-201.

16. Som PM, Curtin HD, Mancuso AA. Imaging-based nodal classification for evaluation of neck metastatic adenopathy. Am J Roentgenol 2000; 174: 837-844.

17. Kao CH, Hsieh JF, Tsai SC, Ho YJ, Yen RF, ChangLai SP, Chieng PU. Comparison of 18F-2-fluoro-2-deoxyglucose positron emission tomography and computed tomography in detection of cervical lymph node metastases of nasopharyngeal carcinoma. Ann Otol Rhinol Laryngol 2000; 109: 1130-1134.

18. Som PM. Detection of metastasis in cervical lymph nodes: CT and MR criteria and differential diagnosis. AJR Am J Roentgenol 1992; 158: 961-969.

19. Don DM, Anzai Y, Lufkin RB, Fu YS, Calcaterra TC. Evaluation of cervical lymph node metastases in squamous cell carcinoma of the head and neck. Laryngoscope 1995; 105: 669-674.

20. Curtin HD, Ishwaran H, Mancuso AA, Dalley RW, Caudry DJ, McNeil BJ. Comparison of CT and MR imaging in staging of neck metastases. Radiology 1998; 207: 123-130.

21. Liu LZ, Zhang GY, Xie CM, Liu XW, Cui CY, Li L. Magnetic resonance imaging of retropharyngeal lymph node metastasis in nasopharyngeal carcinoma: patterns of spread. Int J Radiat Oncol Biol Phys 2006; 66: 721-730.

22. Sakata K, Hareyama M, Tamakawa M, Oouchi A, Sido M, Nagakura H, Akiba H, Koito K, Himi T, Asakura K. Prognostic factors of nasopharynx tumor investigated by MR imaging and the value of MR imaging in the newly published TNM staging. Int J Radiat Oncol Biol Phys 1999; 43: 273-278.

23. Sham JS, Cheung YK, Choy D, Chan FL, Leong L. Computed tomography evaluation of neck node metastases from nasopharyngeal carcinoma. Int J Radiat Oncol Biol Phys 1993; 26: 787-792.

24. Chua DT, Sham JS, Kwong DL, Au GK, Choy DT. Retropharyngeal lymphadenopathy in patients with nasopharyngeal carcinoma. Cancer 1997; 79: 869-877.

25. Lam WW, Chan YL, Leung SF, Metreweli C. Retropharyngeal lymphadenopathy in nasopharyngeal carcinoma. Head Neck 1997; 19: 176-181.

26. Ng SH, Chang JT, Chan SC, Ko SF, Wang HM, Liao CT, Chang YC, Yen TC. Nodal metastases of nasopharyngeal carcinoma: patterns of disease on MRI and FDG PET. Eur J Nucl Med Mol Imaging 2004; 31: 1073-1080.

27. Van den Brekel MW, Stel HV, Castelijns JA, Nauta JJ, van der Waal I, Valk J, Meyer CJ, Snow GB. Cervical lymph node metastasis: assessment of radiologic criteria. Radiology 1990; 177: 379-384.

28. Grégoire V, Levendag P, Ang KK, Bernier J, Braaksma M, Budach V, Chao C, Coche E, Cooper JS, Cosnard G, Eisbruch A, El-Sayed S, Emami B, Grau C, Hamoir M, Lee N, Maingon P, Muller K, Reychler H. CT-based delineation of lymph node levels and related CTVs in the node-negative neck: DAHANCA, EORTC, GORTEC, NCIC, RTOG consensus guidelines. Radiother Oncol 2003; 69: 227-236.

29. Bussels B, Hermans R, Reijnders A, Dirix P, Nuyts S, Van den Bogaert W. Retropharyngeal nodes in squamous cell carcinoma of oropharynx: incidence, localization, and implications for target volume. Int J Radiat Oncol Biol Phys 2006; 65: 733-737.

30. Shimizu K, Inoue H, Saitoh M, Ohtsuki N, Ishida H, Makino K, Amatsu M, Nibu K. Distribution and impact of lymph node metastases in oropharyngeal cancer. Acta Otolaryngol 2006; 126: 872-877.

*Corresponding to

Ming Shu

Department of the Third Surgery

PR China